

## Deposition of Fe<sub>3</sub>O<sub>4</sub> Thin Films by Reactive Magnetron Sputtering and Solid State Reaction

Aleksandras ILJINAS\*, Sigita TAMULEVIČIUS

Department of Physics, Kaunas University of Technology, Studentų 50, LT-51368, Kaunas, Lithuania  
Institute of Physical Electronics of Kaunas University of Technology, Savanorių 271, LT-50131, Kaunas, Lithuania

Received 07 January 2008; accepted 25 February 2008

In this article, we introduce the fabrication of Fe and the Fe<sub>x</sub>O<sub>y</sub> thin films deposited by reactive magnetron sputtering, using facing target sputtering system with Fe planar targets. Also preparation of Fe<sub>3</sub>O<sub>4</sub> thin films using annealing Fe<sub>2</sub>O<sub>3</sub> and Fe multilayer in vacuum is investigated. Crystal structure and phase of as deposited thin films, structural changes of this system after annealing were measured and analyzed using XRD method. The surface morphology was investigated by AFM (Atomic Force Microscopy). Magnetic properties of the samples were measured with the vibrating sample magnetometer (VSM) and MFM (Magnetic Force Microscopy). It was found that the remnant magnetization in Fe<sub>2</sub>O<sub>3</sub>/Fe bi-layer is two times larger than that for Fe<sub>3</sub>O<sub>4</sub>, the coercivity value of bi-layer structure is 5 mT and after annealing it increases up to 10 mT. The resistivity values of thin films were found to be 27 μΩ·cm (Fe) and 85 mΩ·cm (Fe<sub>3</sub>O<sub>4</sub>). The results show that this method is practical for magnetite thin films synthesis because of comparatively low annealing temperature (450 °C) and reasonable annealing time (2 h).

**Keywords:** iron oxides, magnetite, Fe<sub>3</sub>O<sub>4</sub>, facing target sputtering, reactive magnetron sputtering.

### INTRODUCTION

Iron oxide thin films Fe<sub>3</sub>O<sub>4</sub>, γ-Fe<sub>2</sub>O<sub>3</sub>, α-Fe<sub>2</sub>O<sub>3</sub>, have been extensively studied in the past decade because of their unique and interesting magnetic and electrical properties [1–3]. Magnetite, Fe<sub>3</sub>O<sub>4</sub> is conducting with a large degree of spin-polarization at room temperature because there is a gap in the majority spin band at the Fermi level but no gap in the minority spin band. These characteristics of magnetite thin films have a great perspective for spintronic devices [4–9].

The most complicated problem is narrow area of the magnetite phase in a phase diagram of Fe<sub>x</sub>O<sub>y</sub> at temperatures (>1000 °C). Precise control of such parameters as partial pressure of oxygen, substrate temperature and deposition rate must be achieved using reactive deposition of Fe in argon and oxygen ambient. Smallest deviation of this parameters gives such Fe oxide phases as FeO (wustite), α-Fe<sub>2</sub>O<sub>3</sub> (hematite) or γ-Fe<sub>2</sub>O<sub>3</sub> (maghemite) due to excess or deficiency of the oxygen in thin films.

In this article, we introduce the fabrication of the Fe-O thin films deposited by reactive magnetron sputtering combined with post-deposition annealing. The possibility to form magnetite phase using ex-situ annealing of Fe<sub>2</sub>O<sub>3</sub> and Fe multilayer was investigated in our last work and preliminary results are published in [10]. The aim of this work is to summarize the results of the solid state reactions between these layers, deposited by facing target sputtering method and to investigate the composition and structure of the Fe-O thin films.

### EXPERIMENTAL

Fe and Fe<sub>x</sub>O<sub>y</sub> films were deposited on a glass substrate by facing target sputtering (FTS) using magnetron (Fe-

targets) with “off axis” position of substrate [11, 12]. This substrate arrangement enables that the thin films can be deposited avoiding the bombardment by electrons (“damage-free” condition”). Schematic illustration of the facing targets sputtering system used in our research is shown in Fig. 1. The 0.014 m<sup>3</sup>/s rotary pump and 0.5 m<sup>3</sup>/s diffusion pump were used to produce a vacuum. Residual gas pressure was 5·10<sup>-4</sup> Pa. Before the deposition the glass substrates were cleaned using standard procedures: boiling in dimethylformamide and drying in nitrogen. After the chemical treatment all substrates were cleaned using oxygen plasma (5 min at 0.1 Pa) processing. Other deposition parameters are presented in Table 1.

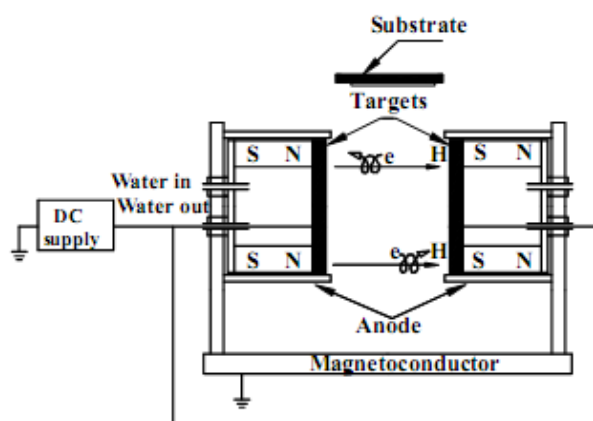


Fig. 1. Schematic illustration of facing targets sputtering system

Table 1. Film preparation conditions

Phase	Fe	Fe <sub>2</sub> O <sub>3</sub>	Fe <sub>3</sub> O <sub>4</sub>
Initial pressure, Pa	5·10 <sup>-4</sup>		
Ar gas pressure, Pa	0.67	–	0.53
O <sub>2</sub> gas pressure, Pa	–	0.67	0.14
Thickness of film, nm	60	500	500

\*Corresponding author. Tel.: +370-61-523668; fax.: +370-37-314423.  
E-mail address: aleksandras.iljinas@ktu.lt (A. Iljinas)

Formed multilayer structures glass/Fe<sub>2</sub>O<sub>3</sub>/Fe, were annealed at 450 °C temperature during 120 min in vacuum (5·10<sup>-4</sup> Pa). Such method is designed for one cycle in vacuum chamber. Deposition rate and thickness of films was monitored by a quartz crystal monitor and by weighing the substrate before and after film deposition with the balance having a resolution of 0.01 mg. The crystalline structure of films was analyzed using a DRON-3M X-ray diffractometer with (Cu-K<sub>α</sub> radiation, λ = 0.15405 nm, Breg-Brentano geometry). The average size of crystallites of thin films was determined from the peak broadening by single line and multiple line analysis using the program WinFit and XFIT. The transmittance and absorption in visible spectrum was measured by a SF-6 spectrophotometer. The single beam scanning was used for the measurement of wavelength ranging from 300 nm to 850 nm. Four-probe method was used to measure the electrical resistivity. Optical spectroscopy was used for optical characteristic measurement. The surface morphologies and magnetic domain structures of the films were studied by atomic force microscope (AFM) and a magnetic force microscope (MFM) DID-3100. Magnetic properties of the samples were measured with the vibrating sample magnetometer (VSM).

## ANALYSIS AND RESULTS

In the first step of the experiment we have investigated the dependence of Fe<sub>x</sub>O<sub>y</sub> phase on oxygen partial pressure in Ar + O<sub>2</sub> ambient. Fig. 2 shows the dependence of the magnetron discharge voltage on the oxygen partial pressure when the discharge current and total pressure are constant. One can see the hysteresis loop dependence, when the discharge voltage is decreased by changing the oxygen partial pressure. In this range of pressure all main Fe<sub>x</sub>O<sub>y</sub> phases: FeO, Fe<sub>3</sub>O<sub>4</sub> and Fe<sub>2</sub>O<sub>3</sub> are formed on the substrate. The XRD pattern analysis of as deposited in Ar ambient thin film shows the phase of Fe material with well expressed peak, corresponding to (110) orientation of crystallites (Fig. 4, a). In Ar + O<sub>2</sub> ambient, where oxygen partial pressure is more then 0.27 Pa, α-Fe<sub>2</sub>O<sub>3</sub> thin film is formed. Energy band gap determined by optical spectroscopy measurements for these films was 2.18 eV.

The optical band gap of the α-Fe<sub>2</sub>O<sub>3</sub> films is calculated from the absorption rate spectra by assuming a parabolic

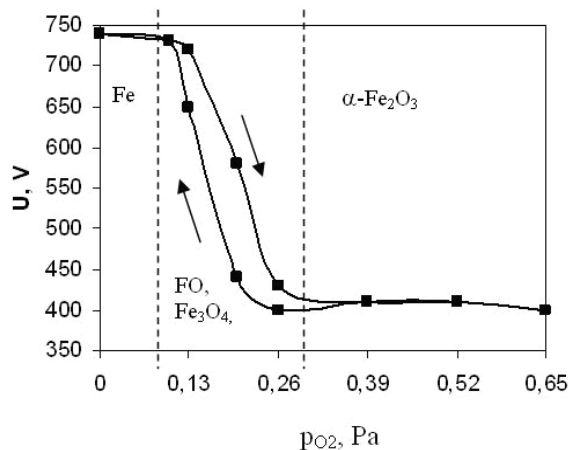


**Fig. 2.** The dependence of the discharge voltage on the oxygen partial pressure ( $I = 1$  A; total pressure  $p = 0.67$  Pa)

band structure for the material. The relationship between absorption coefficient and optical band gap can be expressed as  $\alpha h\nu = A(h\nu - E_g)^{1/N}$ , where  $E_g$  is the band gap energy and  $\alpha$  is the absorption coefficient corresponding to frequency  $\nu$ . The constant  $N$  depends on the nature of electronic transition. In the case of  $\alpha$ -Fe<sub>2</sub>O<sub>3</sub> films,  $N$  is equal to 2 for direct allowed transition. The optical band gaps of hematite were determined by extrapolating the linear portion of the curve from the plot of  $(\alpha h\nu)^2$  versus  $h\nu$ . Fig. 3 show the calculated results. The XRD pattern analysis (Fig. 4, b) of as deposited Fe oxide film shows polycrystalline structure of Fe<sub>2</sub>O<sub>3</sub> phase with the peaks, corresponding to (104) and (110) dominating orientation of hematite phase.

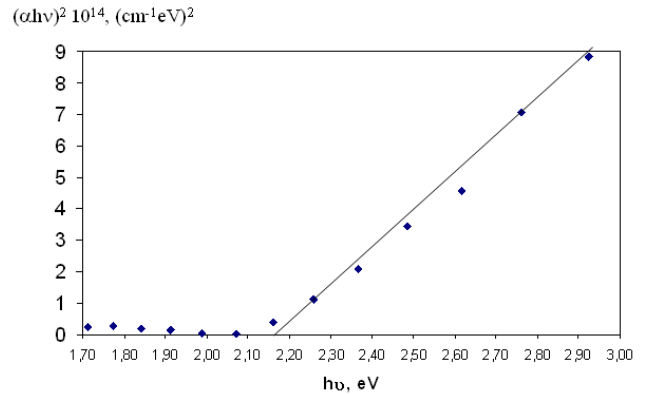
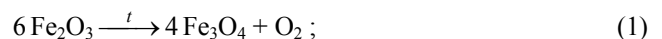


**Fig. 3.** Dependence of the optical band gap of Fe<sub>2</sub>O<sub>3</sub> films prepared on glass substrate

AFM picture shows rather flat surface with some defects for Fe film (Fig. 5, a). Fig. 5, b, AFM picture of Fe<sub>2</sub>O<sub>3</sub> shows rougher surface, than Fe. Roughness as seen is approximately 200 nm. In a range of 0.1 Pa–0.27 Pa of partial oxygen pressure mixed phase films of FeO and Fe<sub>3</sub>O<sub>4</sub> are formed. It was found that Fe thin film very fast oxidizes to Fe<sub>2</sub>O<sub>3</sub> by heating it in atmosphere at low temperature 200 °C. It was impossible to produce Fe<sub>3</sub>O<sub>4</sub> phase by oxidizing Fe thin film in air. The easiest way to produce Fe<sub>3</sub>O<sub>4</sub> is use of solid state reaction in vacuum. In this case there are two possibilities [13–15]: first is oxygen reduction from Fe<sub>2</sub>O<sub>3</sub> via heating in vacuum:

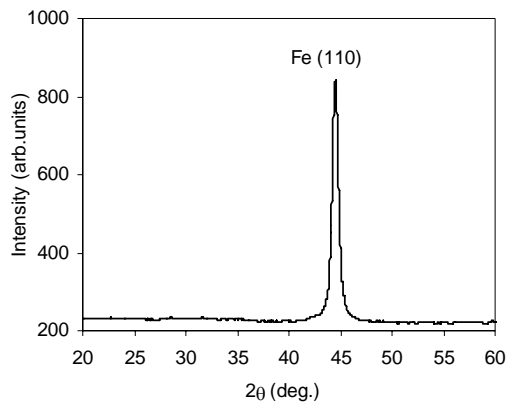


second is mixing and reduction Fe<sub>2</sub>O<sub>3</sub>/Fe multilayer heating at relatively low temperature in vacuum:

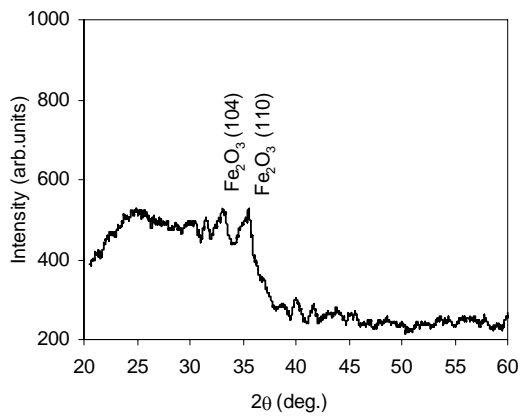


The first reaction needs long time and high enough temperature. In this work we have chosed, the second method (Eq. 2).

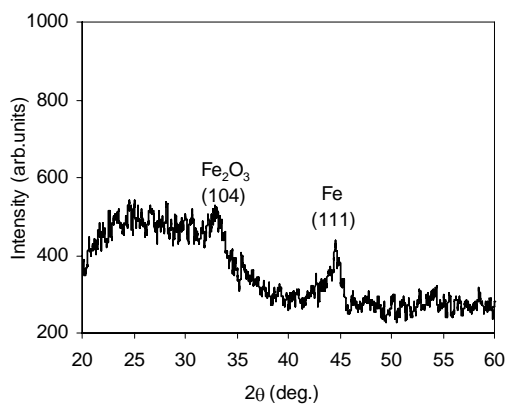
After the determination of deposition parameters for the Fe and Fe<sub>2</sub>O<sub>3</sub> thin films deposition, the bi-layer Fe<sub>2</sub>O<sub>3</sub>/Fe structure was formed. The XRD diffraction patterns of the bi-layer structure are presented in (Fig. 4, c). They show that the positions of the Bragg peaks correspond to (104) orientation of hematite and (111) of iron. The thickness of separate layers was determined from the magnetite phase formation reaction equation (2). It is easy to evaluate that 4 mol of Fe<sub>2</sub>O<sub>3</sub> and 1 mol of Fe could be reduced and mixed to yield 3 mol of Fe<sub>3</sub>O<sub>4</sub>. According to (Eq. 2) for stoichiometric magnetite phase forming the



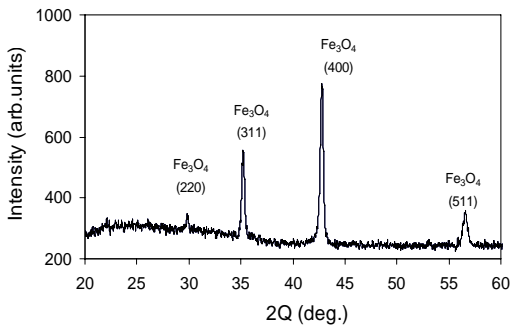
a



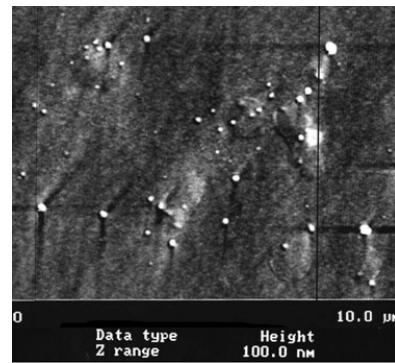
b



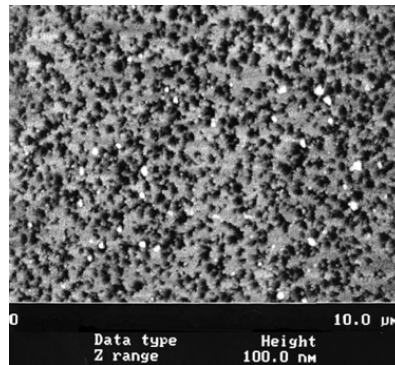
c



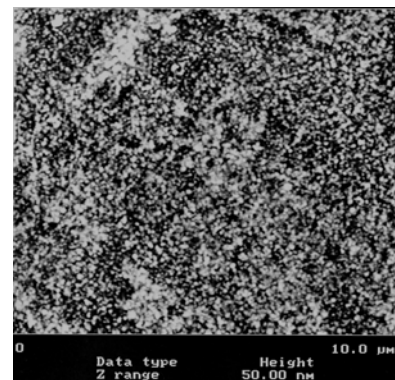
d



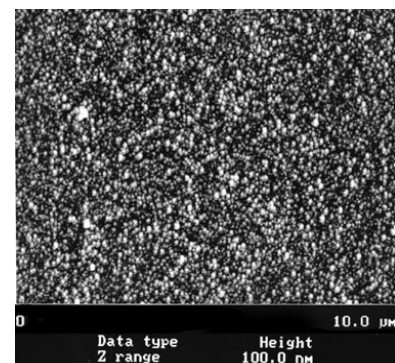
a



b



c



d

**Fig. 4.** XRD patterns for Fe and Fe-O thin films on glass substrates: a – Fe; b –  $\text{Fe}_2\text{O}_3$ ; c –  $\text{Fe}_2\text{O}_3/\text{Fe}$ ; d –  $\text{Fe}_3\text{O}_4$

**Fig. 5.** AFM surface view of as deposited Fe and Fe-O thin films on glass substrates: a – Fe; b –  $\text{Fe}_2\text{O}_3$ ; c –  $\text{Fe}_2\text{O}_3/\text{Fe}$ ; d –  $\text{Fe}_3\text{O}_4$

$\text{Fe}_2\text{O}_3$  and Fe mass ratio is 11.4. The thickness of separate layers was 500 nm for  $\text{Fe}_2\text{O}_3$  and 60 nm for Fe. As deposited the multilayer structures were annealed in vacuum during 120 min time. After the annealing the XRD pattern shows new phase appearance in the annealed structure, which was identified as a magnetite phase (Fig. 3, d). The crystallite size, determined from the XRD peak broadening by single line and multiple line analysis, shows that the mean size of crystallites is 30 nm. AFM image accordingly to XRD shows grained structure of the surface consisted of 20 nm–40 nm grains (Fig. 5, d). These facts illustrate that oxygen reduction reaction and phase transition took place in this bi-layer system. As revealed by the structural analyses of Fe and FeO thin films preparation process, two different magnetic structures can be deposited in the form of  $\text{Fe}_2\text{O}_3/\text{Fe}$  bi-layer and synthesized  $\text{Fe}_3\text{O}_4$  by annealing. In Fig. 6 room temperature hysteresis loops of the  $\text{Fe}_2\text{O}_3/\text{Fe}$  bi-layer and  $\text{Fe}_3\text{O}_4$  samples are given to demonstrate changes of the magnetic structure. Two ferromagnetic rectangular loops illustrate with very different magnetic properties of the layers. The coercivity value of bi-layer structure is 5 mT and after annealing it increases up to 10 mT. The remnant magnetization in  $\text{Fe}_2\text{O}_3/\text{Fe}$  bi-layer is two time larger than that for  $\text{Fe}_3\text{O}_4$ . Because  $\alpha\text{-Fe}_2\text{O}_3$  is non-magnetic material so that for Fe atoms, are responsible for ferromagnetic properties in bi-layer structure.

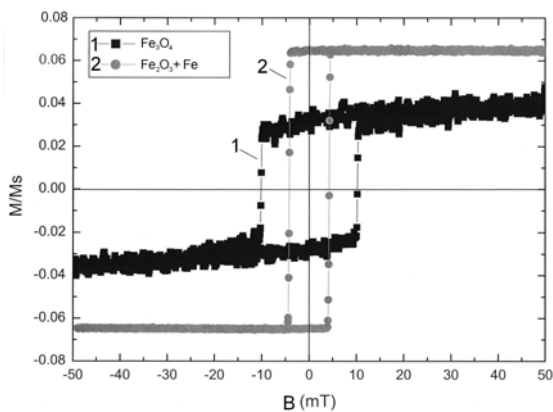
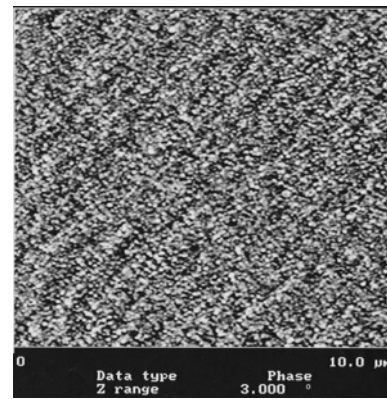


**Fig. 6.** Room-temperature magnetization curves of as formed: 1 –  $\text{Fe}_2\text{O}_3/\text{Fe}$  bi-layer and 2 –  $\text{Fe}_3\text{O}_4$  on glass substrate. ( $M/M_s$  – the ratio of thin films remanent magnetization and saturation magnetization)

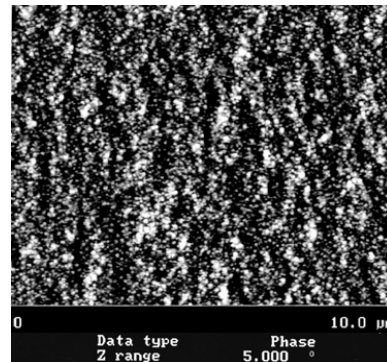
The magnetic microstructure of bi-layer structure and magnetite samples are shown in Fig. 7.

Both of the samples show MFM images with weak contrast, indicating the low magnetic particle concentration and low perpendicular anisotropy in the films. In this view it is difficult to separate any magnetic elements (domains) because of influence of surface morphology.

The electrical conductivity measurements were performed on Fe,  $\text{Fe}_2\text{O}_3$  and  $\text{Fe}_3\text{O}_4$  films deposited on glass substrate by four-probe method. The resistivity values of thin films were found to be  $27 \mu\Omega\cdot\text{cm}$  (Fe) and  $85 \text{ m}\Omega\cdot\text{cm}$  ( $\text{Fe}_3\text{O}_4$ ). The resistivity value is very large because  $\alpha\text{-Fe}_2\text{O}_3$  is dielectric. These values are close to ones of iron and magnetite thin films [13–16].



a



b

**Fig. 7.** MFM surface view of as deposited films: a –  $\text{Fe}_2\text{O}_3/\text{Fe}$  (5 mT), b –  $\text{Fe}_3\text{O}_4$  (10 mT)

## CONCLUSIONS

1. It was shown that  $\alpha\text{-Fe}_2\text{O}_3$  thin film can be produced by reactive magnetron sputtering in  $\text{Ar} + \text{O}_2$  ambient where oxygen partial pressure is higher than 0.27 Pa and deposition rate is 0.6 nm/s.
2. Magnetron bi-layer deposition ( $\text{Fe}_2\text{O}_3/\text{Fe}$ ) with the following thermal annealing enables to produce new magnetite phase with the mean size of crystallites 30 nm.
3. The remnant magnetization in  $\text{Fe}_2\text{O}_3/\text{Fe}$  bi-layer is at least two times larger than that for  $\text{Fe}_3\text{O}_4$ . The coercivity value of bi-layer structure is 5 mT and after annealing increases up to 10 mT. The resistivity values of thin films were found to be  $27 \mu\Omega\cdot\text{cm}$  (Fe) and  $85 \text{ m}\Omega\cdot\text{cm}$  ( $\text{Fe}_3\text{O}_4$ ). These values are close to ones of polycrystalline iron and magnetite thin films. The resistivity value is very large because  $\alpha\text{-Fe}_2\text{O}_3$  is dielectric material.
4. Preparation of  $\text{Fe}_3\text{O}_4$  thin films using annealing  $\text{Fe}_2\text{O}_3$  and Fe multilayer in vacuum is practically acceptable because of comparatively low annealing temperature ( $450^\circ\text{C}$ ) and reasonable annealing time (2 h).

## Acknowledgments

Support of the Lithuanian Sciences and Studies Foundation is acknowledged.

## REFERENCES

1. **De Groot, R. A., et al.** New Class of Materials: Half-Metallic Ferromagnets *Physic Review Letters* 350 1989: pp. 2024.
2. **Coey J. M. D., Berkowitz, A. E.** Magnetoresistance of Magnetite *Physics Review Letter* 72 1998: pp. 734.
3. **Cornell, R. M., Schwertmann, U.** The Iron Oxides: Structure, Properties, Reactions, Occurrences and Uses *Wiley-VCH, Weinheim*, 2nd edition, 2003.
4. **Wolf, S. A., et al.** Spintronics: A Spin-Based Electronics Vision for the Future *Science* 294 2001: pp. 1488 – 1495.
5. **Daughton, J. M.** GMR Applications *Journal of Magnetism and Magnetic Materials* 192 Issue 2 1999: pp. 334 – 342.
6. **Sousa, R. C., Prejbeanu, I. L.** Non-volatile Magnetic Random Access Memories (MRAM) *Comptes Rendus Physique* 6 Issue 9 2005: pp. 1013 – 1021.
7. **Mahesh, G., Stuart, S., Parkin, P.** Magnetic Tunnel Junctions – Principles and Applications *Vacuum* 74 Issues 3–4 2004: pp. 705 – 709.
8. **Jiles, D. C.** Recent Advances and Future Directions in Magnetic Materials *Acta Materialia* 51 2003: pp. 5907 – 5939.
9. **Robbes, D.,** Highly Sensitive Magnetometers *A review Sensors and Actuators A: Physical* 129 Issues 1–2 2006: pp. 86 – 93.
10. **Ilijinas, A., Brucas, R, Stankus, V., Dudonis, J.** Synthesis of Fe<sub>3</sub>O<sub>4</sub> Thin Films by Solid State Reactions *Materials Science and Engineering C* 25 2005: pp. 590 – 594.
11. **Ilijinas, A., Dudonis, J., Brucas, R., Meskauskas, A.** Thin Ferromagnetic Films Deposition by Facing Target Sputtering Method *Nonlinear Analysis: Modelling and Control ISSN:1392-5113* 10 (1) 2005: pp. 57 – 64 .
12. **Ilijinas, A., Bubelis, A., Meškauskas, A., Stankus, V., Dudonis, J.** Facing Target Sputtering System for Ferromagnetic Thin Film Deposition *Lithuanian Journal of Physics* 43 (6) 2004: pp: 463 – 467.
13. **Sivakov, V., Petersen, C., Daniel, C., Shen, H., Mucklich, F., Mathur, S.** Laser Induced Local and Periodic Phase Transformations in Iron Oxide Thin Films Obtained by Chemical Vapor Deposition *Applies Surface Science* 2005: pp. 513 – 517.
14. **Chiba, M., Moriob, K., Koizumi, Y.** Microstructure and Magnetic Properties of Iron Oxide Thin Films by Solid Reaction *Journal of Magnetism and Magnetic Materials* 239 2002: pp. 457 – 460.
15. **Kim, K., Moon, D., Lee, S., Jung, K.** Formation of a Highly Oriented FeO Thin Film by Phase Transition of Fe<sub>3</sub>O<sub>4</sub> and Fe Nanocrystallines *Thin Solid Films* 360 2000: pp. 118 – 121.
16. **Maruyama, T., Shinyashiki, Y.** Iron-iron Oxide Composite Thin Films Prepared by Chemical Vapour Deposition from Iron Pentacarbonyl *Thin Solid Films* 333 1998: pp. 203 – 206.